Electronic cigarette aerosol particle size distribution measurements

Bradley J. Ingebrethsen, Stephen K. Cole & Steven L. Alderman

informa
healthcare

RESEARCH ARTICLE

Electronic cigarette aerosol particle size distribution measurements

Bradley J. Ingebrethsen[1], Stephen K. Cole[2], and Steven L. Alderman[2]

[1]*Department of Chemistry, Medical Technology and Physics, Monmouth University, West Long Branch, NJ, USA and*
[2]*R. J. Reynolds Tobacco Company, Winston-Salem, NC, USA*

Abstract
The particle size distribution of aerosols produced by electronic cigarettes was measured in an undiluted state by a spectral transmission procedure and after high dilution with an electrical mobility analyzer. The undiluted e-cigarette aerosols were found to have particle diameters of average mass in the 250–450 nm range and particle number concentrations in the 10^9 particles/cm^3 range. These measurements are comparable to those observed for tobacco burning cigarette smoke in prior studies and also measured in the current study with the spectral transmission method and with the electrical mobility procedure. Total particulate mass for the e-cigarettes calculated from the size distribution parameters measured by spectral transmission were in good agreement with replicate determinations of total particulate mass by gravimetric filter collection. In contrast, average particle diameters determined for e-cigarettes by the electrical mobility method are in the 50 nm range and total particulate masses calculated based on the suggested diameters are orders of magnitude smaller than those determined gravimetrically. This latter discrepancy, and the very small particle diameters observed, are believed to result from almost complete e-cigarette aerosol particle evaporation at the dilution levels and conditions of the electrical mobility analysis. A much smaller degree, ~20% by mass, of apparent particle evaporation was observed for tobacco burning cigarette smoke. The spectral transmission method is validated in the current study against measurements on tobacco burning cigarette smoke, which has been well characterized in prior studies, and is supported as yielding an accurate characterization of the e-cigarette aerosol particle size distribution.

Keywords: Electronic cigarette, aerosol, particle size, light scattering, spectral transmission

Introduction

Although the use of electronic cigarettes (e-cigarettes) has become increasingly prevalent in recent years, reliable measurements of the particle size distribution of the aerosol produced by these devices, an important physical property for the assessment of respiratory dosimetry, have not been heretofore available. Most e-cigarettes produce a visible, exhalable aerosol, although advertising claims and a developed common parlance have created some confusion regarding the physical state of the effluent. Some sales literature makes claims that only vapor is produced, while the e-cigarette user community has adopted the moniker of "vapers", to describe those who use "vaping" devices. On a technical level, this incorrectly implies that only gas phase material is produced.

The observation of visually detectable light scattering from the effluent unambiguously establishes the presence of a particulate phase. The scarcity of information on particle size for e-cigarettes is due not only to their newness, but also as a result of technical obstacles to the measurement of particle size in high number concentration aerosols containing volatile particulate material. The objective of the present study is to describe a methodology for the measurement of the particle size distribution and number concentration of e-cigarette aerosols and to report measurements on the aerosol produced by two commercially available e-cigarettes.

A wide variety of so-called e-cigarettes have been marketed, most of which employ a similar evaporation/condensation process for transporting material to the

user. The frequent use of the term "atomizer" for the vaporization region of an e-cigarette is another technical inaccuracy as atomization is usually reserved for the process of mechanical dispersion of particulate matter, as opposed to the formation of particles by evaporation/condensation. Most contemporary devices operate in a similar manner. A lithium-polymer or similar battery powers a heating element that is in direct contact with or in very close proximity to an aerosol former solution. Varying proportions of propylene glycol and glycerin commonly make up the bulk of the aerosol former solution, which is typically held within a fibrous solid substrate material located in the e-cigarette mouthpiece section. Some type of wicking mechanism is required to transport the aerosol former solution from the porous reservoir material to the heating element region. The heating element is usually a metal filament coiled around a wick bundle. Some part of this wick is in contact with the aerosol former reservoir material. Only a small fraction of the aerosol former contained within the e-cigarette is vaporized during one puff.

The heating element may be integrated within the mouthpiece section or it may be located as a separate component between the battery and mouthpiece section of the device. Electronic cigarettes are activated with either an automatic flow sensor switch or a manual push button-switch. When powered on, i.e. during puffing, the heating element achieves sufficient temperature to vaporize the aerosol former solution. Ambient air drawn in via inlet ports carries the vaporized components away from the heating element where the vapor cools and condenses to form liquid particulate matter droplets suspended in predominately ambient air. This aerosol is then drawn out the mouthpiece.

This e-cigarette aerosol formation process is in principle similar to that taking place in a burning tobacco cigarette, with the difference that the e-cigarette evaporation takes place at much lower temperatures, which are conditions that likely result in less decomposition and reaction of the vaporized material, and therefore produce an aerosol with many fewer chemical components.

A discussion of the obstacles presented by high number concentration and volatile particulate matter to the measurement of the particle size distribution of tobacco burning cigarette smoke is presented in a recent study by Alderman and Ingebrethsen (2011). These complications are exacerbated for e-cigarettes, due to comparably large number concentrations, as will be shown, and the even higher volatility of the particulate material (formed largely from propylene glycol, glycerin and water). Measurement procedures requiring dilution of the aerosol are expected to result in significant particulate matter evaporation and alteration of the particle size distribution from that provided to the user.

One reported attempt to measure the particle size of e-cigarette aerosol almost certainly suffered from significant particulate matter evaporation during the high dilutions required for measurement with an electrical

mobility analyzer resulting in the observation of very small count average particle sizes for e-cigarette aerosol particles, less than 50 nm (Laugesen, 2009). Using a fast-mobility particle sizer, Schripp et al. (2012) measured the particle size distribution of e-cigarette aerosol under two experimental conditions: (i) aerosol puffed directly from the cigarette mouthpiece into a 10 L chamber with associated dilution; and (ii) aerosol exhaled by a smoker and diluted into an 8 m³ chamber. Evidence was observed of a predominant small diameter mode in the size distribution at about 50 nm on a count basis, similar to the Laugesen (2009) results, and a less populated, larger mode at around 100–200 nm. The larger particles were observed to disappear with ageing and with increased temperature, suggesting that significant evaporation was taking place under the sampling conditions on a minutes-time-scale.

The current study employs a procedure based on the measurement of the wavelength dependence of transmitted light intensity through the aerosol, termed spectral extinction, with best-fit comparisons to theoretical calculations. Kerker (1969) discusses the use of the wavelength dependence of turbidity as a method for the determination of particle size in dispersions. These latter procedures are suitable for dispersions with narrow size distributions of small particles, generally in the Rayleigh scattering range, and of known total mass concentrations. Such an approach is not directly applicable to the current system of interest. Cox and Morgan (1987) applied an analysis procedure to spectral extinction measurements that determined the surface average diameter and number concentration of undiluted mainstream cigarette smoke. This latter methodology requires knowledge of the particulate matter refractive index and the identification of a linear region in an extinction coefficient vs. inverse wavelength plot of the measurements. The Cox and Morgan approach was explored for the current study, but found not to be generally applicable to the data obtained.

The spectral extinction approach employed here determines a best-fit lognormal distribution and particulate matter refractive index by comparison of experimental measurements to a range of theoretical calculations, thus determining a "solution" to the inverse data problem. It is similar to the method that uses the angular dependence of polarization ratios to determine best-fit distribution parameters as described by Kerker (1969), for the general case, and employed by Ingebrethsen (1986a) specifically for cigarette smoke particle size distribution measurements. The current approach determines both size distributions and number concentrations, and is applied to e-cigarette and tobacco burning cigarette aerosols. Additionally, spectral transmission results are compared to size measurements of the same aerosols made with an electrical mobility analyzer and subjected to the required high dilution levels, and further assessed relative to gravimetric filter collections of total particulate matter. The spectral transmission methodology requires no dilution

of the aerosol, thus eliminating potential artifacts from particulate matter evaporation, and provides a time-dependent profile of particle size distribution and number concentration during a puff.

Experimental

The experimental apparatus employed is depicted schematically in Figure 1. A computer controlled puffing machine, previously described by Ingebrethsen and Alderman (2011), was used to draw puffs of specified flow rate profile through the smoking devices. The effluent was drawn directly and continuously through a cylindrical 2.0 mm diameter transmission cell arranged perpendicularly with a white light source beam from a tungsten/halogen high intensity lamp (Ocean Optics, Dunedin, FL). Transmitted light intensity is measured by a linear diode array spectrometer (Ocean Optics) which is connected to the transmission cell, along with the light source, by fiber optic cables. The transmitted light intensity is measured at 10 Hz for four, 6 nm wide wavelength widows centered at 550, 650, 750 and 850 nm.

Two e-cigarettes, a rechargeable model (Brand A), and a disposable model (Brand B), were studied along with one tobacco burning cigarette, Kentucky reference cigarette 3R4F. These e-cigarettes were similar in that both were of the "cartomizer" design type, with the mouthpiece section containing a porous reservoir saturated with the aerosol precursor solution and a metal filament heater coiled around a wick bundle. Three puff profiles were employed for each e-cigarette type: square wave puffs of 55 cm³ total volume for 2, 3 and 4 s total duration. After one "warm-up" puff and a 30 s interval, transmission measurements were made on two puffs at 30 s
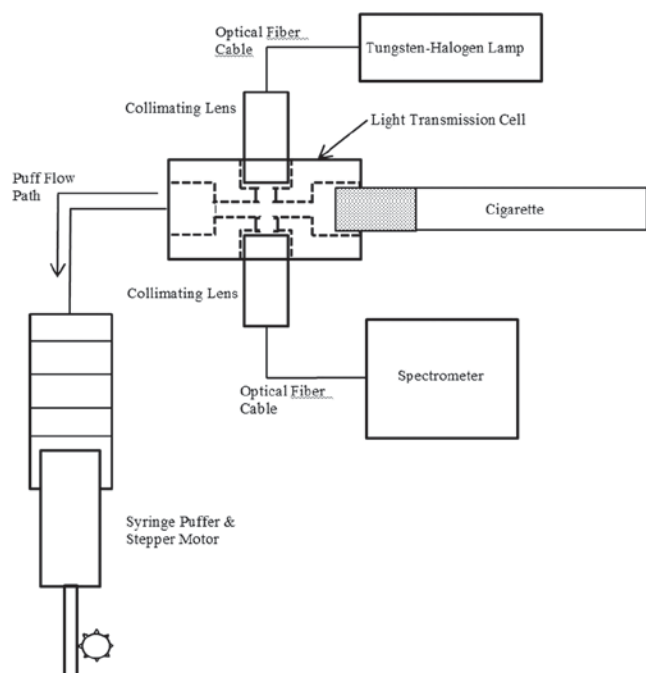
intervals for each of five separate e-cigarette replicates at each puff profile. This yielded 10 puffs at each puff profile for each of the two e-cigarette types. Electronic cigarettes were recently purchased and unused prior to testing. The battery of the Brand A e-cigarette was fully charged prior to conducting experiments; however, it was not possible to charge the disposable Brand B.

The tobacco burning cigarettes were smoked at two puff profiles, 35 cm³ volume with a 2 s duration at 60 s interval and 55 cm³ volume with a 2 s duration at 30 s interval. Five replicates for puff number two and five replicates for puff number five were analyzed separately for particle size from samples taken from five separate cigarettes.

Each product type and puffing regimen combination studied by spectral transmission was also evaluated with a Cambustion differential mobility spectrometer (DMS500) coupled with a Cambustion Smoking Cycle Simulator (SCS). The DMS500 classifies particles in the 5–1000 nm range according to their electrical mobility and aerosol is introduced into the spectrometer via the SCS. The DMS500, SCS, and general data analysis procedures employed here have been described previously. (Symonds et al., 2007; Alderman & Ingebrethsen, 2011). It is worth noting that the particle size distribution descriptors provided by the DMS500 do not assume a form for the distribution, but rather are calculated discretely based on the bin sizes and particle counts. However, aerosol per puff mass was calculated by converting discretely determined geometric mean diameters (d_g) to diameters of average mass (d_{AM}) via a Hatch-Choate equation, implicitly assuming that a log-normal distribution of sizes is appropriate. This log-normal assumption has previously been shown to be a valid for tobacco burning cigarettes (Adam et al., 2009; Alderman & Ingebrethsen, 2011), and is also a good approximation for the present DMS500 derived e-cigarette distributions.

The DMS500 electrometers were set to a low gain mode and the internal rotating disc diluter was set to maintain a dilution ratio of 200:1. SCS-generated square wave puff profiles were employed for the DMS500 evaluations. Aerosol dilution during these measurements takes place both at the SCS sampling head and also at the internal rotating disc diluter. The combined dilution ratios ranged from 3400:1 to 5500:1, depending on the smoking regimen under study. Three consecutive puffs were taken from each e-cigarette; however, the first puff was not analyzed. As with the spectral transmission experiments, five replicates were averaged for each cigarette type and smoking regimen combination. Gravimetric measurements were made using a standard Cambridge filter pad procedure using the same puff engine used for the spectral transmission experiments. The products and samplings procedures for the gravimetric measurements were identical to those employed for the spectral transmission and DMS500 measurements including control of relative humidity during the smoking and weighing procedures.

Figure 1. Apparatus for spectral transmission measurements of aerosol particle size distribution and number concentration.

The same five replicate sets of each e-cigarette type were used for all measurements, i.e. spectral transmission, electric mobility, and gravimetric. Thirty puffs in total were taken per e-cigarette. Previous puff-by-puff measurements revealed no significant changes in aerosol puff mass or number concentration as a function of puff number over this range.

Data Analysis

The transmitted light intensity, $I(\lambda)$ at wavelength λ, depends on the path length through the aerosol, b, the particle extinction coefficient, $k(\lambda)$, and the particle number concentration, N, by

$$I(\lambda) = I_o(\lambda)e^{-k(\lambda)Nb} \qquad (1)$$

or

$$A(\lambda) = k(\lambda)Nb \qquad (2)$$

where $I_o(\lambda)$ is the incident light intensity and $A(\lambda) = ln(I_o(\lambda)/I(\lambda))$ is the absorbance. For a distribution of homogeneous spheres the extinction coefficient is a function of the size parameter $\alpha = 2\pi r/\lambda$, where r is the particle radius, the extinction efficiency, $Q(n,\alpha)$ or $Q(n,r,\lambda)$, where n is the refractive index, and the normalized particle size distribution number density function, $p(r)$. The extinction efficiency is the ratio of the amount of light removed from the incident light beam by a particle to the amount geometrically incident on the particle. The total amount of light removed from the beam per particle is then the product of the particle cross sectional area and the extinction efficiency. Thus the extinction coefficient at a given wavelength and refractive index can be calculated by the following integration

$$k(\lambda) = \int_0^\infty Q(n,r,\lambda)p(r)\pi r^2 dr \qquad (3)$$

The ratios of absorbances at different wavelengths are seen to be equal to the ratios of extinction coefficients at those wavelengths for a given particle size distribution, number concentration and path length

$$\frac{A(\lambda_1)}{A(\lambda_2)} = \frac{k(\lambda_1)}{k(\lambda_2)} \qquad (4)$$

The best-fit size distribution and refractive index was taken to be the combination that yielded the smallest sum of the squares of the differences between the ratios of measured absorbances and the ratios of theoretical extinction coefficients for these parameters at three wavelength ratios, 550 nm/650 nm, 750 nm/650 nm and 850 nm/650 nm.

The aerosol particle size distribution was described by the lognormal distribution function characterized by a geometric mean diameter, d_g, and a geometric standard deviation, σ_g. The theoretical extinction coefficient ratios for each wavelength pair were calculated by a Mie scattering code for ranges of d_g, σ_g, and n. Theoretical calculations were made for d_g from 10 to 700 nm in 10 nm

increments and for σ_g from 1.20 to 1.50 in 0.05 increments. The ranges of refractive index used were different for the e-cigarettes, n from 1.33 to 1.48 in 0.01 increments, and the tobacco burning cigarettes 1.49–1.54 in 0.01 increments. The e-cigarette refractive index range was selected to span the region covering pure water to pure glycerin and including that for pure propylene glycol. The tobacco burning refractive index range corresponds to reported values for mainstream smoke refractive index (McRae, 1982).

Once the best-fit size distribution was determined, the corresponding extinction coefficients at each wavelength were used with the measured absorbances at those wavelengths and the cell path length in equation 2 to calculate the number concentration N in particles/cm³. Thus four measures of number concentrations, one for each wavelength, were calculated for each size distribution determination. The four number concentration calculations were found to be in close agreement and a single average value is reported here for each size distribution determination.

Particle mass concentrations at each point during the puff were calculated from the size distribution and number concentration values and the total particulate mass for the entire puff was calculated by summing the mass concentration by incremental volume products over the puff duration. Mass concentrations were calculated using a diameter of average mass, d_{AM}, which was calculated from the measured d_g and σ_g using the Hatch-Choate relationship

$$d_{AM} = d_g \exp\left(1.5 ln^2 \sigma_g\right) \qquad (5)$$

In order to convert the calculated particle volume to particle mass a density (ρ) of 1.0 g/cm³ was assumed for the tobacco burning cigarette smoke and of 1.1 g/cm³ for the e-cigarette smoke. The value for the e-cigarette density is an approximate estimate based on the assumption that the particulate matter is a mixture of higher density glycerin (1.26 g/cm³) with lower density water (1.0 g/cm³) and propylene glycol (1.04 g/cm³). The mass concentration in grams per cubic centimeter is given by

$$c_g = N\rho\frac{\pi}{6}d_{AM}^3 \qquad (6)$$

Puff-averaged number concentration and diameter of average mass were calculated from the total particulate mass and total number of particles for a puff. Geometric mean diameters were then recalculated using a single, best-fit σ_g and the Hatch-Choate relationship.

Results

Tables 1–3 list the results for the spectral transmission, electrical mobility and gravimetric experiments for all cigarettes and smoking regimens studied. All data reported in Tables 1–3 are puff-averaged values with the indicated standard deviations. Average particle diameters

Table 1. Comparison of per-puff average particle diameter, number concentration and total particulate mass for a 3R4F Kentucky Reference cigarette at two different smoking regimens and puff numbers.

Puff type	Measurement (units)	Transmission	DMS500	Gravimetric
35 cm³/2 s	N_p (cm^{-3} × 10⁹)	0.64 ± 0.32	1.21 ± 0.15	na
	d_{AM} (nm)	373 ± 13	266 ± 12	na
Puff 2	d_g (nm)	337 ± 12	217 ± 8	na
	M_T (mg/puff)	0.60 ± 0.27	0.42 ± 0.03	0.75 ± 0.41
35 cm³/2 s	N_p (cm^{-3} × 10⁹)	1.28 ± 0.41	1.79 ± 0.18	na
	d_{AM} (nm)	331 ± 11	251 ± 8	na
Puff 5	d_g (nm)	289 ± 10	205 ± 6	na
	M_T (mg/puff)	0.84 ± 0.23	0.51 ± 0.07	1.02 ± 0.25
55 cm³/2 s	N_p (cm^{-3} × 10⁹)	1.38 ± 0.42	3.14 ± 0.36	na
	d_{AM} (nm)	390 ± 18	227 ± 11	na
Puff 2	d_g (nm)	253 ± 15	185 ± 8	na
	M_T (mg/puff)	0.94 ± 0.19	1.07 ± 0.16	1.40 ± 0.18
55 cm³/2 s	N_p (cm^{-3} × 10⁹)	2.75 ± 0.91	3.88 ± 0.32	na
	d_{AM} (nm)	270 ± 15	227 ± 11	na
Puff 5	d_g (nm)	228 ± 13	184 ± 8	na
	M_T (mg/puff)	1.52 ± 0.38	1.31 ± 0.20	1.88 ± 0.32

d_{AM}, diameter of average mass; d_g, geometric mean diameter; M_T, total particulate matter mass; N_p, aerosol number concentration.

Table 2. Comparison of per-puff average particle diameter, number concentration and total particulate mass for the Brand A e-cigarette at three different smoking regimens.

Puff type	Measurement (units)	Transmission	DMS500	Gravimetric
55 cm³/4 s	N_p (cm^{-3} × 10⁹)	3.12 ± 1.07	4.10 ± 2.03	na
	d_{AM} (nm)	458 ± 28	24 ± 2.6	na
	d_g (nm)	386 ± 24	18 ± 1.6	na
	M_T (mg/puff)	9.0 ± 1.7	0.0017 ± 0.0006	5.80 ± 0.55
55 cm³/3 s	N_p (cm^{-3} × 10⁹)	2.68 ± 0.51	6.04 ± 1.03	na
	d_{AM} (nm)	402 ± 14	23 ± 1.9	na
	d_g (nm)	339 ± 12	17 ± 0.93	na
	M_T (mg/puff)	5.5 ± 0.70	0.0022 ± 0.0003	4.1 ± 0.39
55 cm³/2 s	N_p (cm^{-3} × 10⁹)	1.8 ± 0.49	8.38 ± 1.26	na
	d_{AM} (nm)	351 ± 23	19 ± 1.7	na
	d_g (nm)	296 ± 19	14 ± 0.68	na
	M_T (mg/puff)	2.4 ± 0.63	0.0019 ± 0.0006	2.5 ± 0.28

d_{AM}, diameter of average mass; d_g, geometric mean diameter; M_T, total particulate matter mass; N_p, aerosol number concentration.

Table 3. Comparison of per-puff average particle diameter, number concentration and total particulate mass for the Brand B e-cigarette at three different smoking regimens.

Puff type	Measurement (units)	Transmission	DMS500	Gravimetric
55 cm³/4 s	N_p (cm^{-3} × 10⁹)	3.71 ± 1.75	5.00 ± 0.98	na
	d_{AM} (nm)	365 ± 64	49 ± 8.8	na
	d_g (nm)	329 ± 58	34 ± 6.9	na
	M_T (mg/puff)	4.8 ± 0.39	0.021 ± 0.013	3.2 ± 0.24
55 cm³/3 s	N_p (cm^{-3} × 10⁹)	5.94 ± 2.73	7.36 ± 1.38	na
	d_{AM} (nm)	303 ± 59	39 ± 9.7	na
	d_g (nm)	265 ± 52	28 ± 7.1	na
	M_T (mg/puff)	4.3 ± 0.51	0.016 ± 0.010	2.3 ± 0.19
55 cm³/2 s	N_p (cm^{-3} × 10⁹)	1.56 ± 0.72	11.8 ± 1.98	na
	d_{AM} (nm)	272 ± 29	29 ± 4.5	na
	d_g (nm)	238 ± 26	21 ± 3.1	na
	M_T (mg/puff)	0.95 ± 0.35	0.010 ± 0.005	1.4 ± 0.20

d_{AM}, diameter of average mass; d_g, geometric mean diameter; M_T, total particulate matter mass; N_p, aerosol number concentration.

(d_g and d_{AM}), number concentrations and total particulate masses are reported as determined by the indicated methods. Table 1 gives the data for the tobacco burning, 3R4F cigarette for the two smoking regimens employed with the second and fifth puffs tabulated separately. Table 2 lists results for the Brand A e-cigarette for the three smoking regimens studied. The values shown are averages over the 10 puffs taken, two per cigarette, for five

separate cigarettes. Table 3 shows the same summary for the Brand B e-cigarette. Not shown in Tables 1–3 are the best fit σ_g values obtained from the spectral transmission data analysis, which in every case ranged between 1.3–1.4. These σ_g values are comparable to those indicated by the current DMS500 measurements (also not provided in table form), as well as to those obtained in previous studies (Adam et al., 2009; Alderman & Ingebrethsen, 2011).

The time-based spectral transmission measurements provide intra-puff profiles of the various aerosol parameters. Figure 2 is a plot of the diameter of average mass and the number concentration vs. time for the 55 cm³/4 s puffing of the Brand A e-cigarette. The values plotted are the average of 10 measurements, 2 puffs each on 5 separate cigarettes taken at this one puffing regimen. Figure 3 is a similar plot for the Brand B cigarette puffed under the same conditions. Figure 4 shows the same parameters plotted vs. time for the fifth puff of the tobacco burning cigarette smoked at the 55 cm³, 2 s duration and 30 s interval puffing regimen. The values plotted are averages for five replicate puffs.

The particle number concentration and size distribution profiles are used to calculate particle mass concentrations profiles. Figure 5 shows the particulate mass concentration in grams per cubic centimeter plotted vs. time for the Brand A cigarette for 55 cm³ puffs taken at 2, 3 and 4 s puff duration. The values plotted are averages of 10 replicate puffs, 2 each per five separate cigarettes. Figure 6 shows the corresponding data plotted for the Brand B cigarette for the same three puffing regimens with the same averaging procedure. Figure 7 is a plot of the mass concentration vs. time for the tobacco burning cigarette for the fifth puff taken at 55 cm³ volume, 2 s duration and 30 s puff interval. The values in Figure 7 are averages over five replicate puffs.

The best-fit refractive indices as determined by the size distribution fitting procedure are plotted vs. time in Figure 8 for the 55 cm³ 4 s puff on the Brand A cigarette. The values plotted are the averages of 10 replicate puffs,
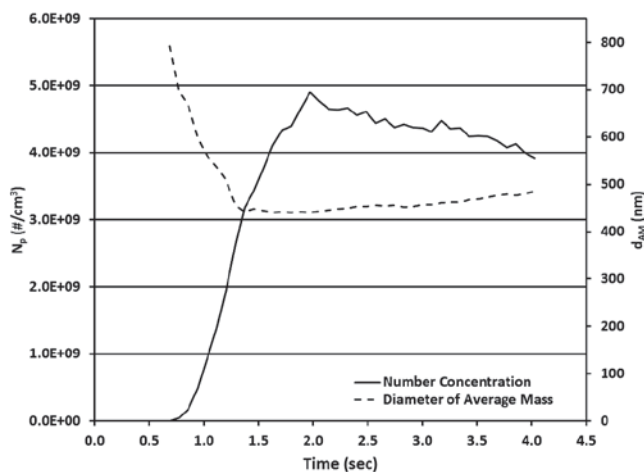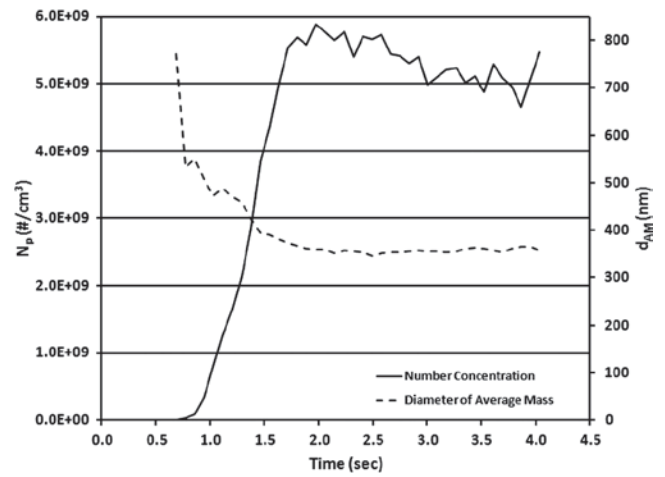

Figure 3. Number concentration and diameter of average mass vs. time for the Brand B ecigarette produced with a 55 cm³ puff volume over 4 s puff duration.
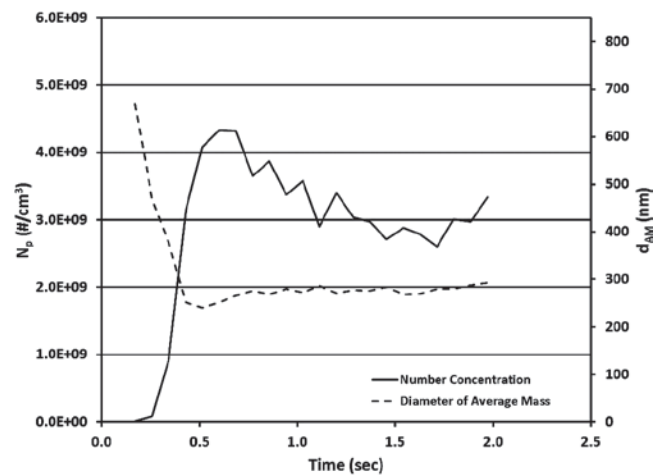

Figure 4. Number concentration and diameter of average mass vs. time for the fifth puff of a 3R4F tobacco burning cigarette puffed at 55 cm³ puff volume, 2 s puff duration and 30 s puff interval.
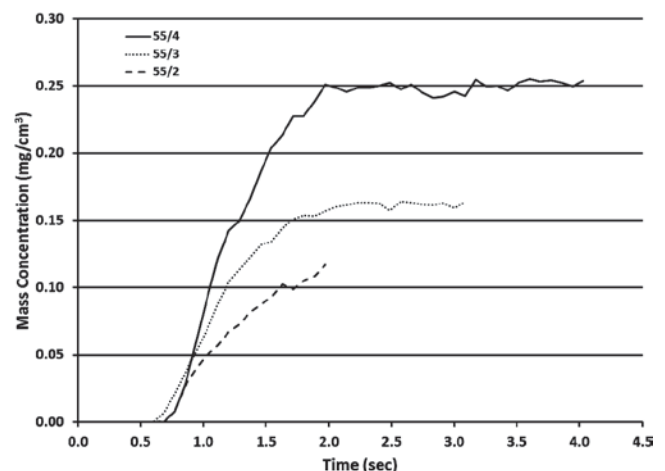

Figure 2. Number concentration and diameter of average mass vs. time for the Brand A e-cigarette produced with a 55 cm³ puff volume over 4 s puff duration.

Figure 5. Particulate mass concentration vs. time for the Brand A ecigarette puffed at a 55 cm³ volume for 2, 3 and 4 s duration.
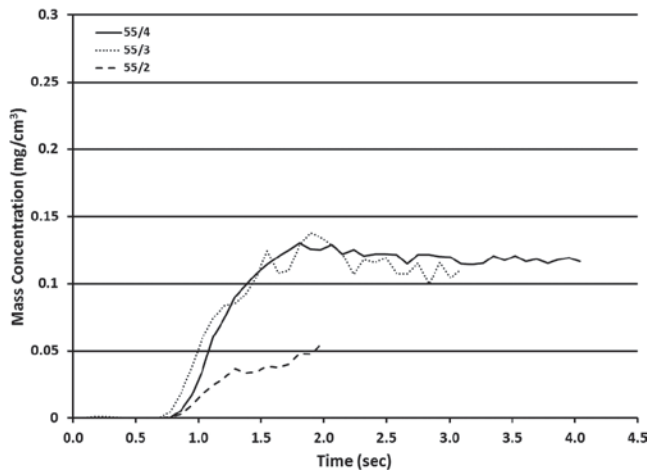
Figure 6. Particulate mass concentration vs. time for the Brand B ecigarette puffed at 55 cm³ puff volume for 2, 3 and 4 s puff duration.
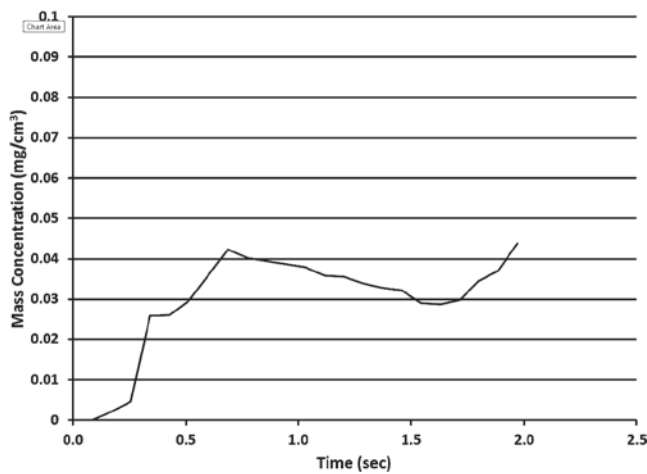

Figure 7. Particulate mass concentration vs. time for the fifth puff of a 3R4F tobacco burning cigarette puffed at 55 cm³ puff volume for 2 s puff duration.

Figure 8. Best-fit refractive index and particulate mass concentration vs. time for the Brand A ecigarette puffed at 55 cm³ puff volume for 4 s puff duration.

Figure 9. Best-fit refractive index and particulate mass concentration vs. time for the Brand B ecigarette puffed at 55 cm³ puff volume for 4 s puff duration.

2 puffs each on 5 separate cigarettes. A plot of the same parameters for the Brand B cigarette is given in Figure 9.

Discussion

The accuracy of the spectral transmission method for particle size and number concentration measurements was assessed by comparison of the transmission results to those from parallel DMS500 electrical mobility determinations on tobacco burning cigarette smoke in light of a prior study of the DMS500 procedure (Alderman & Ingebrethsen, 2011). A review of Table 1 indicates that for the tobacco burning cigarettes, the puff-averaged number concentrations determined by the transmission measurements agree within approximately a factor of two with those determined by the DMS500 procedure. The average particle diameter is in even better agreement (factor of ~1.4) between the transmission and the DMS500 procedure as is the calculated total particulate mass (factor of ~1.35). As determined in the earlier study by comparison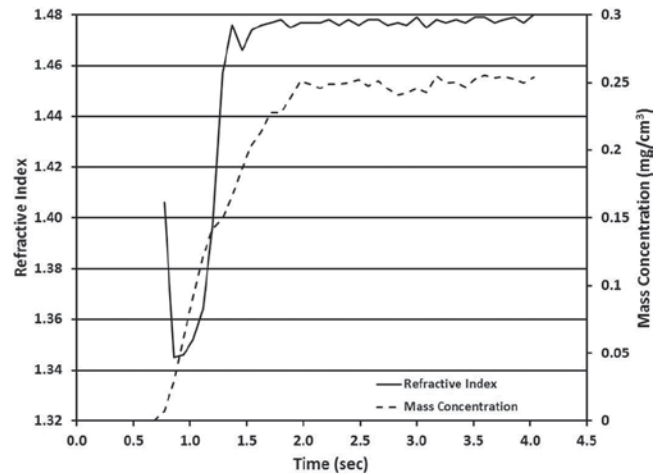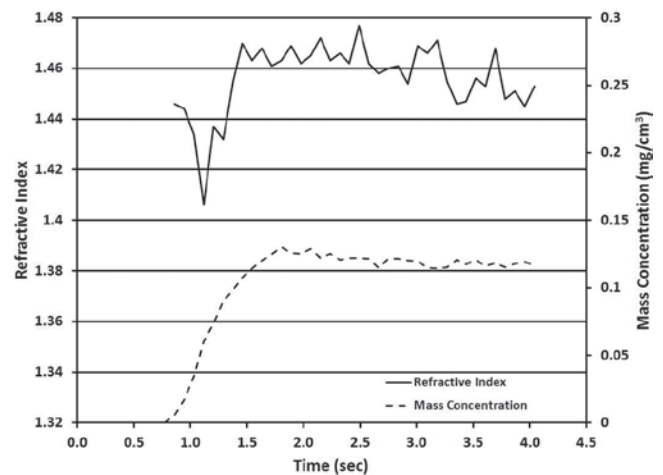 of DMS500 determined total particulate mass and gravimetric filter mass (Alderman & Ingebrethsen, 2011), some degree of particle evaporation of tobacco burning cigarette smoke takes place in the DMS500 due to dilution. Estimates of the extent of average size reduction due to this evaporation for the data in Table 3 suggest an actual size of about 10–25% larger than the uncorrected size reported by the DMS500 bringing the transmission measurement and the DMS values into slightly better agreement. The transmission procedure eliminates the need for dilution of the aerosol, thereby avoiding distortion of the size distribution by evaporation during the measurement. The size and number concentration determinations by the transmission procedure appear to be in reasonable agreement with the DMS500 and gravimetric measurements which are, in turn, in good agreement with prior studies of the particle size of mainstream tobacco smoke (Bernstein, 2004; Ingebrethsen, 1986b).

The average sizes determined by the DMS500 measurements for the e-cigarette aerosol, Tables 2 and 3, are dramatically smaller than those measured by the

transmission procedure and are similar to those reported previously using a similar electrical mobility procedure that also required high smoke dilution levels (Laugesen, 2009). The computed per puff total particulate masses calculated from the transmission data are in reasonable agreement with the gravimetrically determined values for the e-cigarettes. In contrast, the DMS500-derived per-puff particulate masses are observed to be orders of magnitude smaller than those from the gravimetric filter collections, confirming the suspected high degree of evaporation during electrical mobility measurements.

The aerosol exiting the e-cigarettes studied is believed to be accurately represented by the sizes and number concentrations listed in Tables 2 and 3. Use of the size distribution parameters determined by the transmission procedure would be expected to provide a significantly more accurate starting point for dosimetry calculations that the much smaller, and much more highly diffusing, particle sizes suggested by the high dilution electrical mobility methods. The 100–200 nm particle diameter mode reported by Schripp et al. (2012) for diluted e-cigarette aerosol that is observed to disappear with aging and increased temperature may be the last remnants of a fresh aerosol closer in size to that reported here. This hypothesis suggests that the smaller particle diameter mode observed by Schripp is comprised of residue particles.

The average particle sizes of the aerosols from the two types of e-cigarettes evaluated in this study are comparable to each other and to that of fresh mainstream tobacco burning cigarette smoke although some differences are worth noting. Across the puffing regimes studied, the diameter of average mass for the Brand A electronic cigarette measured by transmission is about 30% larger than that for Brand B. In contrast, the diameter of average mass for Brand A from the electrical mobility procedure, possibly indicating the size of residue particles as discussed above, is smaller than that for Brand B by about a factor of one half. Comparing each cigarette type across all respective puffing regimes, the Brand A diameter of average mass is observed to be slightly larger by about 10% than that for the tobacco burning aerosol while Brand B is measured to be slightly smaller, about 15%, than the tobacco burning smoke average size. Given the complex aerosol dynamics expected during the inhalation of high concentration, volatile aerosols of these types, discussed below, any implications of these trends and magnitudes of differences will require further study and analysis. Number concentrations and per puff total particulate masses for the e-cigarette aerosols are also found to be similar to those of tobacco burning smoke.

The accuracy of the particle sizes indicated by the transmission measurements is also supported by a qualitative assessment of aerosol light scattering efficiencies and coagulation rates. The e-cigarette smoke appears, qualitatively, to scatter an amount of visible light approximately equal to that of tobacco burning smoke (the transmission measurements actually reveal that the Brand A aerosol scatters more light, i.e., has a higher optical density than the tobacco burning cigarette smoke

studied). If the e-cigarette aerosol particles were in fact as small as the electrical mobility measurements suggest, the theoretical light scattering efficiency (per mass of particulate matter) would be less than 1% that of the tobacco burning cigarette smoke studied. That is, the e-cigarette aerosol would be predicted to have much fainter visibility than is observed. Similarly, to account for the total particulate mass measured gravimetrically for the e-cigarette aerosol if the particulate matter were dispersed as 40 nm particles, the number concentration would have to be in the greater than 10^{11} particles per cubic centimeter range. This high number concentration would correspond to an extremely high Brownian coagulation rate which would rapidly grow the particles to significantly larger sizes.

It should be emphasized that the particle size distributions reported here for the e-cigarette aerosols correspond to the aerosol as it exits the cigarette. As is the case for tobacco burning mainstream smoke, the e-cigarette aerosol is expected to be dynamic after puffing and during inhalation. Both the size and number concentration are expected to evolve and are subject to the possible effects of condensational growth, particulate matter evaporation, coagulation and particle deposition (Ingebrethsen, 1986b). In fact, the high hygroscopicity and volatility of the particulate matter in the e-cigarette aerosol might yield an even more dynamic system than tobacco burning mainstream smoke. The present report does not address the dynamics of the e-cigarette aerosol during puffing and inhalation; however, an accurate analysis of the inhalation dynamics begins with an accurate description of the input aerosol properties. Such a description, we believe, is provided by the current measurements.

The intra-puff time resolution of the transmission measurements provides some insight to the functioning of the e-cigarettes studied and a preliminary basis for comparison to tobacco burning cigarettes. In all of the intra-puff plots there is an initial delay in the appearance of measureable aerosol attributable to a combination of factors that vary in significance with cigarette type and puff profile. There is a small, 0.1–0.3 second, delay in the commencement of piston movement of the puffing machine after the nominal start of the puff at time zero. For the e-cigarettes there is also some delay in turning on the battery by the flow sensor. For both the e-cigarettes and the tobacco burning cigarette there is a delay attributable to the aerosol generation process after heating begins. Although Figure 2 indicates that Brand A produces a somewhat smaller puff-averaged size than Brand B in Figure 3, both electronic cigarettes generate a similar pattern of low concentrations of larger particles that evolve into a relatively steady state of higher concentrations of smaller particle size. These intra puff patterns are likely related to changes in the aerosol formation conditions during the puff and bear a qualitative similarity to the size and number concentration intra-puff pattern observed for tobacco burning smoke in Figure 4 even though the temperature gradients and vapor generation mechanisms for tobacco burning cigarettes are significantly different in

these combustion based cigarettes than in the electrically heated, lower operating temperature electronic cigarettes.

A comparison of the mass concentration profiles of the Brand A and Brand B e-cigarettes, Figures 5 and 6, to that of the tobacco burning cigarette, Figure 7, suggests the following observations. The initial appearance of measureable aerosol is slightly more delayed for the e-cigarette than for the tobacco burning cigarette. The e-cigarette reaches "steady state" mass concentration levels for the lower velocity flow rates, 55 cm^3 spread over 3 s and 4 s, and not for the higher velocity flow rates, 55 cm^3 for 2. Figures 2–4 suggest some similarity between the e-cigarette and the tobacco burning cigarette number concentration and average size intra-puff profiles in that there is a similar progression from an initial transition period of decreasing size and increasing number concentration to a latter period of relatively stable average size and number concentration. These similarities illustrated in Figures 2–7 are noted in light of the difference in heat input profile between electronic cigarettes and tobacco burning cigarettes. For electronic cigarettes total heat input depends predominantly on the duration of the heater "on-time", approximately the puff duration, in contrast to the heat input profile of tobacco burning cigarettes that depends on the combustion mass consumed during a puff determined by both on the puff duration and the puff volume drawn past the fire cone of the cigarette.

A final observation regarding the type of information available from the spectral transmission measurement is with respect to the intra puff refractive index profiles, Figures 8–9. For the Brand A cigarette profile, Figure 8, and less so for the Brand B profile in Figure 9, there is some indication of particulate mass compositional changes during the puff. Specifically, the dip in refractive index early in the profile toward the value for water, 1.33, and the subsequent plateau at a higher value suggest some differential distillation of the particulate matter forming material during the puff.

Conclusions

The spectral transmission method for particle size determination provides accurate size measurements on e-cigarette aerosols, in large part by eliminating the need for aerosol dilution. The e-cigarette aerosol particles undergo nearly complete evaporation at the dilution levels required for DMS500/SCS electrical mobility size measurements, yielding average particle size values that are significantly smaller than those determined to be present in fresh e-cigarette aerosols. Modeling of respiratory deposition of e-cigarette aerosols will be much more accurately accomplished using the transmission based size distribution measurements reported here than with the much smaller sizes suggested by high dilution electrical mobility determinations that put the average size in a different regime with respect to aerosol dynamics mechanisms. The average particle diameters measured

by the spectral transmission method for the aerosol from two types of electronic cigarettes are, in fact, more comparable to those of tobacco burning cigarette smoke than had been suggested by prior reports that employed high levels of aerosol dilution in the measurements. The current study confirms particle evaporation during high aerosol dilutions in the electrical mobility measurements as the cause of the indication of artificially small particle sizes. Additionally, the intra-puff time resolution inherent in the spectral transmission method yields some insight to the e-cigarette aerosol generation process and suggests some similarities and differences compared to tobacco burning cigarette smoke generation.

Acknowledgements

Declaration of interest

References

Adam T, McAughey J, McGrath C, Mocker C, Zimmermann R. 2009. Simultaneous on-line size and chemical analysis of gas phase and particulate phase of cigarette mainstream smoke. Anal Bioanal Chem 394:1193–1203.

Alderman SL, Ingebrethsen BJ. 2011. Characterization of mainstream cigarette smoke particle size distributions from commercial cigarettes using a DMS500 fast particulate spectrometer and smoking cycle simulator. Aerosol Sci Tech 44:1409–1421.

Bernstein DM. 2004. A review of the influence of particle size, puff volume, and inhalation pattern on the deposition of cigarette smoke particles in the respiratory tract. Inhal Toxicol 16:675–689.

Cox KA, Morgan CH. 1987. Particle size and mass concentration measurements of mainstream tobacco smoke using a light extinction spectrometer. In: Proceeding of the International Conference on the Physical and Chemical Processes Occurring in a Burning Cigarette. April 26–29, Graylyn Conference Center of Wake Forest University, Winston-Salem, NC, USA, 474–488.

Ingebrethsen BJ. 1986a. Evolution of the particle size distribution of mainstream cigarette smoke during a puff. Aerosol Sci Tech 5:423–433.

Ingebrethsen BJ. 1986b. Aerosol studies of cigarette smoke. Rec Adv Tob 12:54–142.

Ingebrethsen BJ, Alderman SL. 2011. Coagulation of mainstream cigarette smoke in the mouth during puffing and inhalation. Aerosol Sci Tech 44:1422–1428.

Kerker M. 1969. The scattering of light and other electromagnetic radiation. New York: Academic Press.

Laugesen M. 2009. Ruyan e-cigarette bench top tests, Poster 5–11. Society for Research on Nicotine and Tobacco, Dublin, April 30.

McRae DD. 1982. The refractive index of individual cigarette smoke droplets. J Colloid Interf Sci 87:117–123.

Schripp T, Markewitz D, Uhde E, Salthammer T. 2012. Does e-cigarette consumption cause passive vaping? Indoor Air. DOI: 10.1111/j.1600-0668.2012.00792.x

Symonds PRJ, Reavell KS, Olfert JS, Campbell BW, Swift SJ. 2007. Diesel soot mass calculation in real-time with a differential mobility spectrometer. J Aerosol Sci 38:52–68.